Stochastic boundary conditions for coastal flow modeling

Arthur J. Mariano,[1] Toshio M. Chin,[1,2] and Tamay M. Özgökmen[1]

Received 22 January 2003; accepted 9 April 2003; published 2 May 2003.

[1] Recent high-resolution radar data of surface velocity between the Florida Current and the coast allow us for the first time to deduce coastal boundary conditions for ocean models based on observations. A stochastic model is found to be a better choice for simulating properties of the observed vorticity than a model with deterministic boundary conditions. A stochastic model parameterizing boundary conditions is developed and embedded in a simple quasigeostrophic ocean model. Comparison of numerical simulations of western boundary flow with stochastic boundary conditions against simulations with traditional no-slip and free-slip conditions reveals significant differences in the formation of coherent mesoscale structures and the energetics of the western boundary current. Coherent structures such as dipoles and submesoscale vortices can be generated using stochastic boundary conditions. The boundary current variability becomes more energetic and ''episodic'' than quasi-periodic circulation features in the simulations using the conventional boundary conditions. *INDEX TERMS:* 4546 Oceanography: Physical: Nearshore processes; 4255 Oceanography: General: Numerical modeling; 4576 Oceanography: Physical: Western boundary currents; 4532 Oceanography: Physical: General circulation. **Citation:** Mariano, A. J., T. M. Chin, and T. M. Özgökmen, Stochastic boundary conditions for coastal flow modeling, *Geophys. Res. Lett.*, *30*(9), 1457, doi:10.1029/2003GL016972, 2003.

1. Introduction

[2] At present, typical grid spacing in ocean general circulation models (OGCMs) for large-scale simulations is on the order of 5–20 km. Subgrid-scale turbulence is typically represented by diffusion operators acting on momentum, which require associated boundary conditions. No-slip (zero tangential velocity) and free-slip (zero stress) boundary conditions are typically used. A linear combination of these types of boundary conditions, or partial slip, was also proposed for ocean general circulation simulations [*Haidvogel et al.*, 1991]. However, such boundary conditions lead to substantially different behavior not only in western boundary currents [e.g., *Özgökmen et al.*, 1997] but also in the basin-wide circulation [e.g., *Böning*, 1986]. Selection of boundary conditions based on physical grounds has been difficult so far, especially when numerical models resolve only the meso-scale motion. For instance, the no-slip condition is an observational fact about the interaction of the fluid with a solid boundary on the molecular level. While it is a well-justified boundary condition for simulations at the scale of laboratory experiments [*Batchelor*, 1967], oceanic motion on the scales of several kilometers does not have to mimic this interaction. Similarly, it is not clear whether small-scale processes within the boundary layer would allow the western boundary currents to slip smoothly along the boundaries, as in the case of free-slip condition. Given that the choice of boundary conditions, or even differences in their numerical implementation [e.g., *Verron and Blayo*, 1996], have a strong impact on numerical simulations of ocean and coastal circulation, the choice of appropriate boundary conditions for ocean models is still an important and outstanding problem [*Carnevale et al.*, 2001].

[3] Typical boundary conditions in ocean models are based on a somewhat arbitrary assumption that sub-mesoscale coastal processes play a rather passive role in the dynamics of boundary currents. This is primarily due to convenience and the lack of comprehensive observations with small enough spatial and temporal scales to resolve the coastal boundary layer. The recent availability of high-resolution surface velocity data along the Florida coast [*Shay et al.*, 2002] and elsewhere provides a strong motivation to revisit this issue with the objective of parameterizing sub-mesoscale boundary layer processes as boundary conditions for ocean general circulation models.

[4] The 4-Dimensional Current Experiment provided accurate velocity data for a 28-day period in July/August, 1999 [*Shay et al.*, 2002; *Peters et al.*, 2002], based on Ocean Surface Current Radar (OSCR) measurements (u, v) over a 7 km $\times$ 8 km area along the southeastern Florida coastline, at horizontal and temporal resolutions of $\sim$250 m and 15 minutes, respectively.

[5] In this study, we conduct a statistical analysis of vorticity with the objective of obtaining proper boundary conditions for numerical circulation models. We show that the boundary vorticity is better characterized as an energetic stochastic process, rather than a steady-state process. A parsimonious stochastic boundary process model is developed and compared to free-slip and no-slip parameterizations using a quasi-geostrophic ocean model.

2. Boundary Vorticity Observations

[6] Relative vorticity $\zeta(x, y, t) = \partial v/\partial x - \partial u/\partial y$ is computed from the OSCR velocity measurements. Figure 1 shows time series of ζ at the three locations examined by *Peters et al.* [2002], which are 1.1 km, 3.6 km, and 7.6 km offshore at a given latitude (26.06°N). Energetic and episodic nature of the near-shore vorticity can be observed, with temporal scales ranging from hours to five days and peak values greater than $10f_0$, where $f_0 \equiv 6.4 \times 10^{-5}$ s^{-1} is the approximate ambient Coriolis frequency. The pattern of alternating vorticity level that appears to be roughly com-

[1]Meteorology and Physical Oceanography, Rosenstiel School of Marine and Atmospheric Science, University of Miami, Miami, Florida, USA.
[2]Also at Jet Propulsion Laboratory, California Institute of Technology, Pasadena, California, USA.

Copyright 2003 by the American Geophysical Union.
0094-8276/03/2003GL016972$05.00

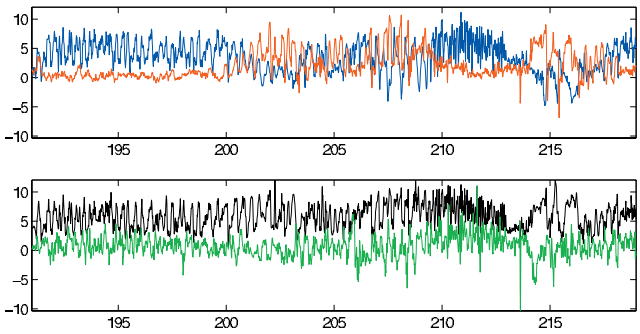

Figure 1. Time series of OSCR-based $\zeta(x, y, t)$ at y = 26.06°N and x = 1.1 km offshore (green), 3.6 km offshore (blue), and 7.6 km offshore (red). The black line is the zonal maximum $\hat{\zeta}(y,t)$. The unit of ζ is 6.4×10^{-5} s^{-1} ($= f_0$). Time axis is in year day, where 190 is 9 July 1999.

plementary to each other between the 3.6 km and 7.6 km points is indicative of meandering of the Florida Current. The dynamics are dominated by such meanders, O(km)-scale cyclonic vortices, and motion energetic at periods of ten hours and twenty-seven hours [*Peters et al.*, 2002; *Shay et al.*, 2002]. Longer temporal scales have also been observed [*Soloviev et al.*, 2003].

[7] To focus on the positive (cyclonic) vorticity of the coastal shear zone and to avoid the over-smoothing by spatial averaging, the maximum vorticity at each latitude y is selected,

$$\hat{\zeta}(y,t) = \max_x \zeta(x,y,t) \tag{1}$$

(black line, Figure 1). One concern in taking the maximum value is that statistical outliers may be incorporated into $\hat{\zeta}(y,t)$. Similar time series obtained by taking several order statistics (the maximum is the "order 1" statistics), however, indicate that obvious outliers are absent, due to editing of the data and the use of a smoothing spline-fit to the velocity data. The e-folding time of the autocorrelation function of $\hat{\zeta}(y,t)$ is about 2 hours. The along-shore mean of the OSCR vorticity can be estimated as the average of $\hat{\zeta}(y,t)$ and is 3.93×10^{-4} s^{-1} ($\approx 6f_0$), with a standard deviation of 1.29×10^{-4} s^{-1}.

[8] The vorticity time series display several prominent periodicities at the sub-daily scales. A power spectral peak at 10-hour period is particularly prominent and is also consistent with the dominant periodicity of 10 hours observed by *Peters et al.* [2002] in the spectra of the velocity components. A stochastic oscillator with a complex frequency $\omega_0 \equiv 2\pi/T + i/\tau$, where $T = 10$ hours is the period and $\tau = 2$ hours is the decay constant, can be used to model this periodicity. A convenient tool to introduce randomness and quasi-periodicity is to model the vorticity as a second-order autoregressive (AR-2) process

$$\zeta_n = a_1\zeta_{n-1} + a_2\zeta_{n-2} + w_n \tag{2}$$

where n is the time index ($t = n\Delta t$) and the coefficients can be given as $a_1 = e^{i\omega_0} + e^{-i\omega_0}$ and $a_2 = -|e^{i\omega_0}|^2 = -1$. The variance of the white-noise Gaussian process w_n is evaluated empirically.

[9] Figure 2a displays a Hovmoeller diagram of $\hat{\zeta}(y,t)$. The pattern of slightly tilted vertical streaks in the figure indicates a relatively constant advection of the vorticity. From the slope of the largest tilt, a northward advection speed of about 0.25 to 0.55 ms^{-1} can be observed. To quantify the advection speed, a lagged correlation $\langle \hat{\zeta}(y,t)\hat{\zeta}(y+\Delta y, t+\Delta t)\rangle$ is evaluated for the fixed time-lag of Δt = 15 minutes (OSCR sampling interval). From the correlation coefficient values, the mean lag Δy is determined to be 231.6 m, from which the mean northward advection speed is estimated to be 0.26 ms^{-1}.

3. A Stochastic Boundary Model

[10] A simple model for vorticity parameterization is proposed. The basic ingredients are the periodicity as captured by the regression (2) and a constant (deterministic) northward advection. Given the advection speed c, the vorticity is determined by the generating function g as

$$\hat{\zeta}(y,t) = g(y - ct), \tag{3}$$

where in general g is a sum of randomly forced periodic oscillators. If there were K frequencies in the model, g is an autoregression process of order $2K$. Here, we consider the case of $K = 1$ using the most dominant of the empirical period of 10 hours. Consideration for a more sophisticated model, such as multiple periodicities and a stochastic advection speed, is deferred for future studies.

[11] The generating function g is evaluated as the sum of the regressive oscillator (2) and a white noise process v which represents (simplistically) the ambient, wide-band spectral energy,

$$\begin{aligned} g'_n &= a_1 g'_{n-1} + a_2 g'_{n-2} + w_n \\ g_n &= g'_n + v_n \end{aligned} \tag{4}$$

where the variances of the driving noise w_n and ambient noise v_n are both obtained empirically as 1.64×10^{-10} s^{-2}, or $(0.2f_0)^2$. A sampling interval of $c\Delta t$ (= 231.6 m) is used for discretization. Figure 2b shows the Hovmoeller diagram of a numerically generated $\hat{\zeta}(y,t)$, while Figure 3 compares the generated and observed vorticity time series. Here, only

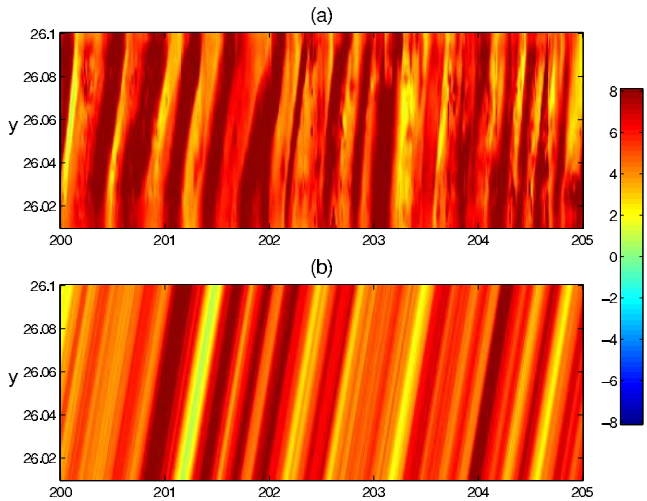

Figure 2. Vorticity magnitude for $\hat{\zeta}(y,t)$ (a) from OSCR measurements and (b) numerical simulation using equations (3) and (4). The unit of the color bar is in 6.4×10^{-5} s^{-1}.

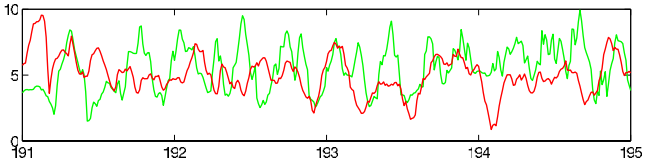

Figure 3. Time series of $\hat{\zeta}(y,t)$ from OSCR measurements (green line) and numerical simulation using equations (3) and (4) (red line). The unit of $\hat{\zeta}$ is f_0. Time axis is in year day.

the fluctuating part of vorticity with zero mean is used as boundary conditions assuming that the large-scale relative vorticity is represented by the ocean model.

4. Numerical Experiments

[12] A reduced gravity, quasigeostrophic model is used to test and compare the different boundary conditions. Using nondimensionalization $\psi = (T_0 H^{-1})\,\psi^*$, $(x, y) = R_d\,(x^*, y^*)$, $t = f_0^{-1} t^*$, where ψ is the streamfunction in the (x, y)-plane, T_0 the net (western boundary current) transport, H the active layer depth, $R_d = \sqrt{g' H}/f_0$ the radius of deformation, and g' the reduced gravity. The model equations are:

$$\frac{\partial q}{\partial t} + a\,J\left(\psi, \nabla^2\psi\right) + b\frac{\partial \psi}{\partial x} = d\nabla^4\psi, \tag{5}$$

$$\nabla^2\psi - \psi = q, \tag{6}$$

where the nondimensional parameters are $a \equiv T_0/(HR_d^2 f_0)$, $b \equiv \beta\, R_d/f_0$ and $d \equiv \nu/(R_d^2 f_0)$, β is the meridional gradient of Coriolis frequency, and ν is horizontal viscosity.

[13] The model is configured in a regular rectangular domain. The meridional length is 3000 km, which is adequate to contain several wavelengths of characteristic instabilities of the western boundary current. The zonal length is 1000 km such that the domain is much wider than the mesoscale eddies and the width has negligible impact on the solution. The reference latitude is 26°, which is the latitude of the radar observations. The equilibrium layer thickness (H = 1000 m) and the stratification ($g' = 0.01$ ms^{-1}) are such that the Rossby radius of deformation is 52 km, typical of midlatitude circulation. The viscosity is taken as $\nu = 400$ m^{2}s^{-1}, which is high enough to ensure numerical stability at the selected grid scale, but also small enough to allow highly-nonlinear dynamics ($a \gg d$). The horizontal grid size is 10 km, which (i) resolves both the mesoscale eddy scale of $R_d = 52$ km, and (ii) the viscous western boundary current scale of $(\nu/\beta)^{1/3}$ = 27 km, and (iii) coincides with the OSCR sampling area size. The model time step of 900 s is not only much smaller than the time it takes for the internal waves to cross grid spacing (~3000 s) or the fastest current to cross the grid (~9000 s), but also corresponds to the OSCR time sampling. The model is forced by specifying a net transport between the eastern and western boundaries. The transport is $T_0 = 30$ *Sv*, which is the average transport of the Florida Current [*Leaman et al.*, 1989]. Periodic boundary conditions are used in the northern and southern boundaries, and free-slip boundary conditions are applied along the eastern boundary.

5. Comparison of Boundary Conditions

[14] The behavior of the system is explored as a function of the boundary conditions along the western boundary:

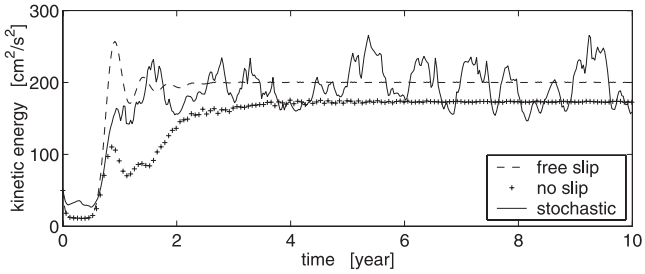

Figure 4. Basin averaged kinetic energy $\langle|\nabla\psi|^2/2\rangle$ (in cm^2 s^{-2}) as a function of the integration time (in years) in the case of free-slip (dashed line), no-slip (line with "+++") and stochastic (solid line) boundary conditions.

free-slip, no-slip, and stochastic boundary conditions based on parameters determined from radar observations and the stochastic boundary model developed in §3. The primary objective is to determine whether the effect of the stochastic boundary conditions remains limited to a thin layer along the boundary, or they can transform the behavior of the western boundary current by generating different coherent structures than those with free-slip and no-slip boundary conditions.

[15] The basin-averaged kinetic energy from experiments with free-slip, no-slip and stochastic boundary conditions are shown in Figure 4. Following a spin-up period of 0.5–1 years, during which the front propagates westward by Rossby advection, there is an adjustment period of 2–3 years during which coherent structures emerge. For free-slip and no-slip cases, these coherent structures show little variability, leading to nearly-constant energy curves during the rest of the integration. The energy level is lower in no-slip than that in free-slip case due to higher dissipation along the western boundary. The case with stochastic boundary conditions, however, exhibits a great degree of variability as soon as the front reaches the western boundary. These fluctuations push the kinetic energy level beyond those obtained from free-slip and no-slip conditions, which indicate the fundamental impact of stochastic boundary conditions on the western boundary current.

[16] Characteristic coherent structures during the equilibrium state of simulations are depicted in Figure 5. The patterns obtained with free-slip and no-slip boundary con-

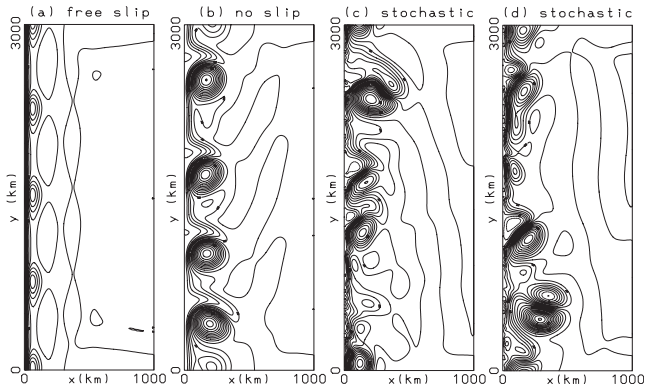

Figure 5. Snapshots of transport streamfunction (contour interval: 5 Sv) illustrating characteristic coherent structures with (a) free-slip, (b) no-slip and (c,d) stochastic (two realizations) boundary conditions.

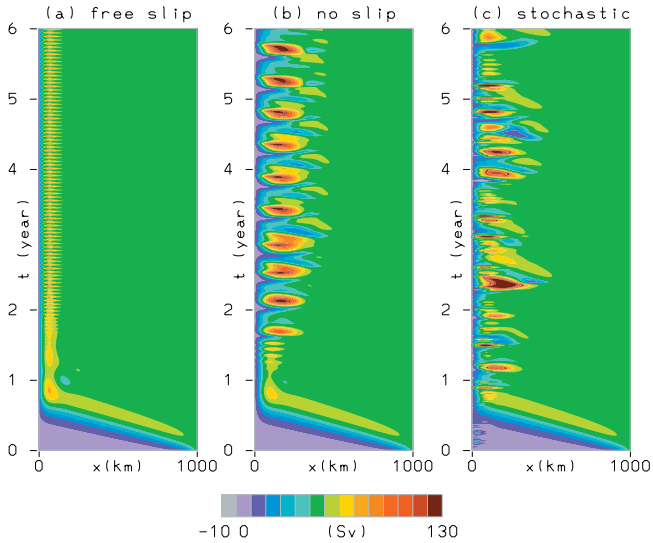

Figure 6. Hovmoeller diagrams of transport streamfunction across the middle of the domain for (a) free-slip, (b) no-slip and (c) stochastic cases for the first 6 years of the numerical integrations.

ditions are identical to those investigated by *Berloff and McWilliams* [1999]. These finite amplitude modes (Figures 5a and 5b) are basically temporally and spatially periodic, and show little variability as they travel northward. In contrast, the flow field with stochastic boundary conditions frequently displays formation of energetic meanders, dipoles, and eddies at a broad-band of scales, as well as no or small perturbations along the western boundary current (Figures 5c and 5d).

[17] The behavior of the coherent structures is viewed from a different perspective by plotting the transport streamfunctions along a zonal section in the middle of the domain as a function of time (Figure 6). Following westward propagation of the front (the average westward speed is 0.05 ms^{-1} in exact agreement with βR_d^2), characteristic coherent structures form in both free-slip and no-slip cases, and propagate northward with little variability. The northward propagation speed is much faster and the coherent structures are smaller in the free-slip case, leading to the high-frequency signal along the western boundary. The structures are slower and larger in the no-slip case. In both cases, the behavior of coherent structures is nearly periodic. The behavior resulting from stochastic boundary conditions can be characterized as "episodic", showing a large range of spatial and time scales during the integration. Overall, it is clear that the use of coastal boundary conditions based on observations leads to a significantly different evolution of the modeled western boundary current than those with conventional boundary conditions.

6. Summary

[18] This study is motivated by fundamental questions that arise from direct application of no-slip condition, which is essentially based on a laboratory scale (few *m*) fluid dynamics, or free-slip condition, which is an ad-hoc argument proposed for larger scale applications, as boundary conditions in ocean models. The recent availability of accurate, near-shore, high-resolution (250 m in space, 15 *min* in time) radar-based velocity data of the boundary layer between the Florida Current and the coast allows us for the first time to deduce closed boundary conditions for ocean circulation models based on observations.

[19] A stochastic model is constructed to parameterize the observed boundary layer vorticity. Comparison to no-slip and free-slip conditions reveals significant differences in the formation of coherent structures and evolution of overall energetics. The empirical variability in the boundary vorticity is thus capable of affecting basin-scale circulation features. The time-evolution of kinetic energy in model simulation is indicative of cascading of small-scale processes up to larger-scale processes, as the random oscillation with periods of years must have been caused by the oscillations in the boundary process that have periods of only hours. Aggregation of the smaller scale processes tends to some "episodic" features lasting for months, as clearly evident in the streamfunction fields.

[20] **Acknowledgments.** The work is supported in parts by the NSF grant OCE-0136700, NOPP grant N00014-99-1-1066, and ONR grants N00014-95-1-0257 and N00014-99-1-0049. The surface current data were acquired under ONR grant N00014-98-1-0818 at University of Miami. This study has benefited greatly from discussions with L. K. (Nick) Shay.

References

Batchelor, G. K., *An Introduction to Fluid Dynamics*, Cambridge Univ. Press, New York, 1967.

Berloff, P., and J. McWilliams, Quasigeostrophic dynamics of the western boundary current, *J. Phys. Oceanogr.*, *29*, 2607–2633, 1999.

Böning, C., On the influence of frictional parameterization in wind-driven circulation models, *Dyn. Atmos. Ocean*, *10*, 63–92, 1986.

Carnevale, G., F. Cavallini, and F. Crisciani, Dynamics boundary conditions revisited, *J. Phys. Oceanogr.*, *31*, 2489–2497, 2001.

Haidvogel, D., J. McWilliams, and P. Gent, Boundary current separation in a quasigeostrophic, eddy-resolving ocean circulation model, *J. Phys. Oceanogr.*, *22*, 882–902, 1991.

Leaman, K. D., E. Johns, and T. Rossby, The average distribution of volume transport and potential vorticity with temperature at three sections across the Gulf Stream, *J. Phys. Oceanogr.*, *19*, 36–51, 1989.

Özgökmen, T. M., E. P. Chassignet, and A. M. Paiva, Impact of wind forcing, bottom topography, and inertia on midlatitude jet separation in a quasigeostrophic model, *J. Phys. Oceanogr.*, *27*, 2460–2476, 1997.

Peters, H., L. K. Shay, A. J. Mariano, and T. M. Cook, Current variability on a narrow shelf with large ambient vorticity, *J. Geophys. Res.*, *107*(C8), 3087, doi:10.1029/2001JC000813, 2002.

Shay, L., T. Cook, H. Peters, A. Mariano, R. Weisberg, P. An, A. Soloviev, and M. Luther, Very high-frequency radar mapping of surface currents, *IEEE J. Oceanic Eng.*, *27*, 155–169, 2002.

Soloviev, A., M. Luther, and R. Weisberg, Energetic baroclinic super-tidal oscillations on the shelf off southeast Florida, *Geophys. Res. Lett.*, *30*, doi:10.1029/2002GL016603, in press, 2003.

Verron, J., and E. Blayo, The no-slip condition and the separation of western boundary currents, *J. Phys. Oceanogr.*, *26*, 1938–1951, 1996.

T. M. Chin, A. J. Mariano, and T. M. Özgökmen, Meteorology and Physical Oceanography, Rosenstiel School of Marine and Atmospheric Science, University of Miami, 4600 Rickenbacker Causeway, Miami, FL 33149, USA. (tchin@rsmas.miami.edu)